

Waveguide electro-optic modulation in micro-engineered LiNbO₃

D Janner¹, D Tulli¹, M Belmonte² and V Pruneri^{1,3}

¹ ICFO—Institut de Ciències Fòniques, Mediterranean Technology Park, 08860 Castelldefels (Barcelona), Spain

² Avanex Corporation Sede Secondaria, San Donato Milanese (MI), Italy

³ ICREA—Institut Català de Recerca i Estudis Avançats, 08010, Barcelona, Spain

E-mail: davide.janner@icfo.es

Received 6 March 2008, accepted for publication 30 May 2008

Published 27 August 2008

Online at stacks.iop.org/JOptA/10/104003

Abstract

In this paper, after describing the basics of LiNbO₃ based integrated electro-optic modulators, we will show how techniques such as etching, domain inversion and thin film processing can be used to realize new geometries which can take the performance to unprecedented levels. In particular we will review recent results on the use of domain inversion on a micron scale to improve the electro-optic response of LiNbO₃ waveguide modulators in terms of bandwidth and driving voltage. These applications of domain inversion techniques might be even more important and commercially valuable than those in nonlinear optics (e.g. quasi-phase-matched optical parametric devices). With respect to standard single-domain structures, larger bandwidths and lower driving voltages can be obtained, thus achieving figure of merits for the electro-optic response that are up to 50% larger. As a demonstration, a chirp-free modulator, having ~2 V switching voltage and bandwidth of 15 GHz, was fabricated by placing the waveguide arms of a Mach–Zehnder interferometer in opposite domain oriented regions. The modulator, as indicated by system measurements, could be driven in a single-drive configuration with inexpensive low-voltage drivers, e.g. SiGe based, typically used for electro-absorption devices.

Keywords: lithium niobate, electro-optic modulators, broadband modulators, domain inversion

(Some figures in this article are in colour only in the electronic version)

1. Introduction

Optical networks as the main carriers of information are continuously growing in importance due to the ever increasing demand in bandwidth. Inside optical transmission systems, high-speed optical modulators are one of the fundamental building blocks. External LiNbO₃ modulators are still extremely effective [1], in particular for long haul and metro applications, as is shown by their recent increasing commercial volume: total worldwide revenue for digital dense wavelength division multiplexed (DWDM) transmission doubled over the last year. Other materials cannot still match LiNbO₃ modulation performance in terms of, for example, extinction ratio, insertion loss, chirp feature, and optical transparency—the latter being particularly important taking into account the increased use of tunable laser sources. With

respect to, for example, semiconductor based modulators, the LiNbO₃ market share could become even larger if performance, integration, and cost further improve. Among others, the required improvements should include at the same time high modulation efficiency (i.e. large modulation bandwidth at low driving voltage) and feasibility of a robust and economic large-scale fabrication process. Indeed, even though the use of velocity matched (VM) traveling wave electrode configurations [1, 2] greatly increases the modulation bandwidth (BW), the potential of LiNbO₃ in terms of modulation efficiency is far from being exploited. In fact the frequency dependent microwave loss limits the bandwidth of VM modulators: the higher the frequency the higher the microwave loss; thus, for a given length L , the effective modulation length becomes smaller at higher frequency, and so does the efficiency. This makes the BW inversely proportional

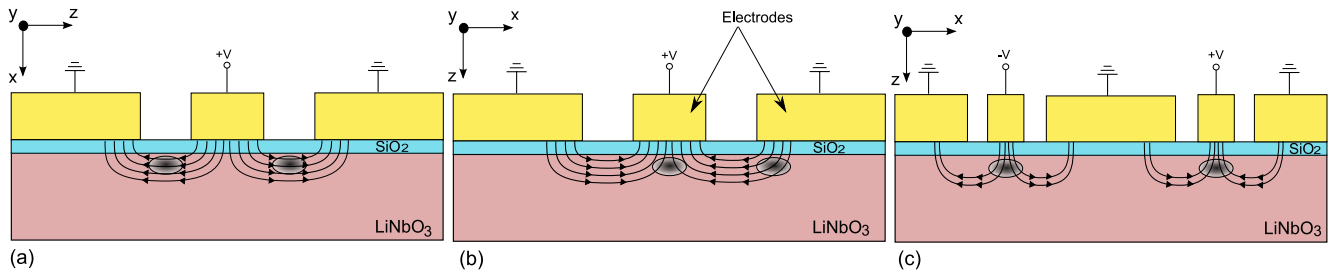


Figure 1. Cross sections of conventional Mach-Zehnder modulators: (a) x -cut single drive, (b) z -cut single drive, (c) z -cut dual drive.

to L , similar to the switching voltage (V_π), so that a trade-off exists between V_π and BW and the ratio BW/V_π is used as a figure of merit. To obtain improved efficiency (increase in BW/V_π), better coupling between the microwave and optical fields is required. Different solutions have been proposed to this end. Thin plate modulator configuration in x -cut crystals [3] and a ridge waveguide [5, 4] in z -cut modulators have been proposed to obtain higher modulating field concentration in the area of the optical field. These solutions, respectively, rely on sophisticated thin film and etching processing, and thus are not ideal, especially in a large-scale production environment.

Domain inversion (DI) in ferroelectrics, such as LiNbO_3 , has been widely exploited in all-optical processes, e.g. quasi-phase-matched second harmonic generation, optical parametric oscillation, and WDM frequency conversion [6–9]. So far, its use in electro-optics has been mostly limited to quasi-velocity-matching devices using periodic structures [10, 11] or to achieve a desired chirp value for high-frequency and broadband modulators [12]. More recently, domain engineering of z -cut LiNbO_3 structures has been proposed to produce large bandwidth and very low-voltage modulators where the push-pull effect in the interferometric structure has been obtained by placing the waveguides in opposite sign electro-optic coefficient regions (i.e. opposite-oriented domains) and under the same electric field [13]. This is in contrast with previous high-frequency modulating structures in single-domain crystals where the two waveguides are placed under two distinct electrodes having different (usually opposite sign) voltages [1]. With respect to previous modulating structures in single-domain crystals, the proposed DI symmetric scheme allows one to achieve maximum efficiency, chirp-free and single-drive operation at the same time.

In this paper we will show how DI micro-engineering in LiNbO_3 is a very effective means to increase the figures of merit for the electro-optic response. As examples we report the design, fabrication, and testing of a DI modulator with 15 GHz bandwidth and ~ 2 V switching voltage, and the design of a 30 GHz modulator having $V_\pi = 4.3$ V. Our recently developed technique for Ti-indiffusion [14] allows for a robust waveguide fabrication and domain inversion process.

The paper layout is as follows. In section 2 we will outline some background concepts on modulator design and performance, which are presented in section 3, together with experimental demonstrations. Finally, in section 4, some conclusions will be drawn.

2. Background

In order to present our results, we summarize the main principles and equations of a traveling wave LiNbO_3 modulator with straight electrodes perfectly impedance matched, 50/50 power splitting [1, 15], and perfect symmetry of the electrical and electro-optical parts between the two arms. In figure 1 we sketch the microwave fields and the cross sections of the basic configurations for (a) a single-drive x -cut modulator, (b) a single-drive z -cut modulator and (c) a dual-drive z -cut modulator. The difference between the z -cut and the x -cut type is the use of optical TM or TE mode, respectively, for the coupling with the RF signal. The difference between the single-drive and dual-drive configuration is the possibility of driving with different voltages (V_1 and V_2) the two arms of the Mach-Zehnder interferometer, although in the following we will consider mainly the case when $V_1 = -V_2$. For these modulators the traveling microwave voltage along each arm can be written as

$$V(z) = V_0 e^{-\alpha(f_m)z} \sin(k_m \delta z - 2\pi f_m t_0), \quad (1)$$

where V_0 is the amplitude of the wave, $k_m = 2\pi n_m / \lambda_m$ is the microwave wavenumber, $\delta = 1 - n_{\text{opt}} / n_m$ is the relative mismatch between the index of refraction of the microwave (n_m) and optical (n_{opt}) waves, f_m is the microwave frequency corresponding to the wavenumber k_m , and t_0 accounts for an initial phase mismatch between the optical and microwave fields. More realistically, we included in equation (1) the microwave losses $\alpha(f) = \alpha_0 \sqrt{f}$ ($\alpha_0 = 0.49$ dB (cm GHz) $^{-1/2}$) occurring during propagation and which we estimated using an FEM program [16]. Driven by the microwave, the phase change experienced by the optical wave at the end of the modulator can be written as

$$\Delta\phi(f_m) = -\frac{2\pi}{\lambda} \frac{n_{\text{opt}}^3}{2} r \frac{\Gamma}{G} \int_0^L p(z) V_0 \sin(k_m \delta z - 2\pi f_m t_0) dz, \quad (2)$$

where L is the length of the arms of the modulator itself, λ is the optical wavelength, r is the electro-optic coefficient (in our case for LiNbO_3 , $r = r_{zz}$), G is the spatial gap between the two electrodes, and Γ is the overlap integral between the optical and microwave electric fields, defined as [2]

$$\Gamma = \frac{G}{V_0} \frac{\int E_m |E_{\text{opt}}|^2 dS}{\int |E_{\text{opt}}|^2 dS}, \quad (3)$$

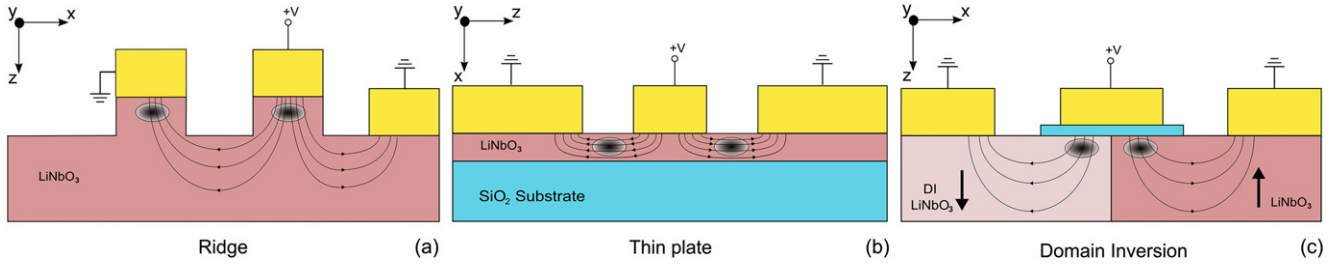


Figure 2. Comparison between different modulator schemes: (a) ridge, (b) thin plate, (c) domain inverted push-pull.

with E_m and E_{opt} being the microwave and optical fields and the integration domain being a plane transversal to the modulator propagation direction. The function $p(z) = \pm 1$ in equation (2) accounts for changes in the electro-optic response along the modulator due to LiNbO₃ domain inversion. Now starting from equation (2), the *electro-optic response* for a single-drive single-domain (unpoled) modulator, having $p(x) = 1$ everywhere, can be defined as the normalized quantity

$$m(f) = \left| \frac{\Delta\phi(f)}{\Delta\phi(0)} \right| = e^{-\frac{\alpha f}{2}} \sqrt{\frac{\sinh^2\left(\frac{\alpha L}{2}\right) + \sin^2\left(\frac{\xi L}{2}\right)}{\left(\frac{\alpha L}{2}\right)^2 + \left(\frac{\xi L}{2}\right)^2}} \quad (4)$$

with $\xi = 2\pi f_m(n_m - n_{opt})/c_0$, c_0 being the speed of light in vacuum. Using equations (2) and (4) we can derive the expression for switching voltage—corresponding to a phase change of π and producing a theoretical zero optical output—and an estimate of the bandwidth (in GHz) for lossless ($\alpha_0 = 0$) propagation:

$$V_\pi = \frac{\lambda G}{2n_{opt}^3 L r \Gamma}, \quad BW_{\alpha=0} = \frac{0.181}{\pi(n_m - n_{opt})L}. \quad (5)$$

This expression shows the inverse dependence on the length of the modulator for BW and V_π . In the case of dual-drive modulators [1], any asymmetry or deviation in the electrodes or waveguide geometry leads to an imbalance in the modulator response, thus introducing a chirp in the modulated signal. This effect is estimated by the chirp parameter η , defined as

$$\eta = \frac{\Gamma_1 - \Gamma_2}{\Gamma_1 + \Gamma_2} \quad (6)$$

where Γ_1 and Γ_2 are the overlap integrals between the optic and microwave fields in the first and the second waveguide arms, respectively. Especially in long haul transmission, the ideal case is when $\eta = 0$. For this reason, besides bandwidth and switching voltage, the chirp parameter is also considered for the applicability in a transmission system of a modulator.

In order to increase the efficiency of a modulator the ratio BW/V_π needs to be increased. The most straightforward way to do this is to increase the overlap integral Γ . To this end, some solutions have been proposed (see figure 2). In these geometries the increased overlap is achieved either through a deformation of the modulating field lines (ridge and thin plate) or the placement of the waveguides under a narrower and more

efficient electrode (DI inverted push-pull). The use of ridge waveguides in z -cut substrates (figure 2(a)) allows deforming the lines of the microwave field so that the component along the z -axis is stronger, thus better exploiting the highest electro-optic tensor element (r_{zz}). The thin plate geometry in x -cut crystals (figure 2(b)) obtains a similar effect. The etching or thin film processing (e.g. polishing, crystal ion slicing, etc) can become critical in LiNbO₃, which is a very hard material. DI is instead a quite developed, reliable, and relatively inexpensive fabrication technique, e.g. in nonlinear optics to achieve quasi-phase-matching, thus making its use well suitable to micro-structure either or both the modulator transversal (figure 2(c)) and longitudinal (see next section) dimensions.

3. Features improvement in micro-structured domain inverted modulators

The design of a modulator comprises the longitudinal (along the propagation) and transversal directions, which can be separately studied [1]. This gives two degrees of freedom in the optimization of modulator performance, in particular using domain micro-structuring via electric field poling, as we propose in the following.

3.1. Reduced switching voltage

Concerning the design along the transverse axis, recently [13] we have demonstrated that by using DI in LiNbO₃, an efficient modulator can be produced. The cross section of the proposed modulator highlighting the working principle is shown in figure 2(c). Note that there is a silica based buffer layer between the hot electrode and the lithium niobate crystal. This layer ensures at the same time low optical loss by keeping the evanescent optical field low in the lossy metal electrodes and velocity matching between the traveling optical and microwave fields. With respect to previous structures of coplanar waveguide (CPW) modulators [1, 12] the proposed layout offers several advantages, summarized in table 1, and with respect to the other approaches illustrated in figure 2, it offers greater feasibility, even though not the same performances. Driving voltages (for similar device length) are close to those offered by dual-drive structures (two waveguides under two hot electrodes driven by opposite sign voltages), with the advantage of being single drive, and hence in the absence of any synchronization issue between two microwave lines. On the other hand, the typical single-drive structure

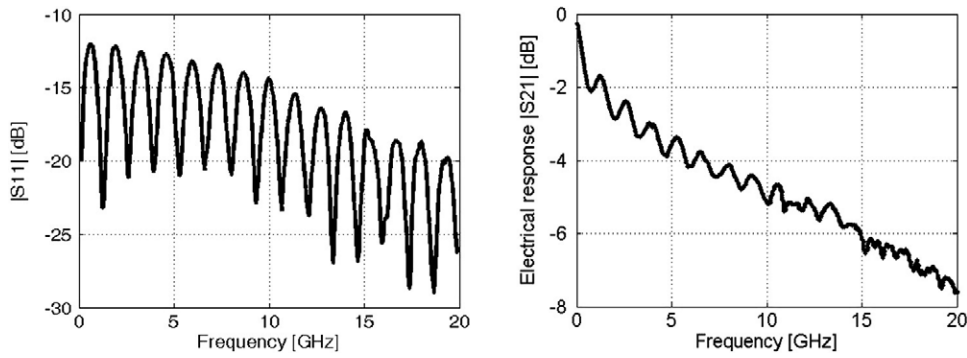


Figure 3. Domain engineered (as in figure 2(c)) modulator electrical reflection ($|S_{11}|$) and electrical response ($|S_{21}|$).

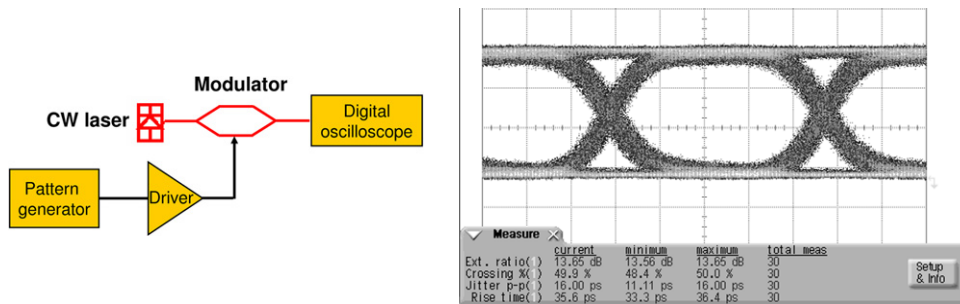


Figure 4. Test setup (left) and eye diagram measurements showing wide opening at 10 Gb s^{-1} (right).

Table 1. Comparison of the performances of different configurations.

Structure	$V_{\pi}L$ (V cm)	Γ	Chirp (α)	RF drive
LiNbO ₃ physical limit	≈ 3.6	1	0	Single
Standard CPW [1]	≈ 12	0.3	$\neq 0$	Single
Dual drive CPW [1]	≈ 8	0.45	Arbitrary($=0$)	Dual
CPW with longitudinal DI [12]	≈ 12	0.3	≈ 0	Single
Domain inverted push-pull	≈ 9	0.4	0	Single
Ridge [5, 4]	≈ 6	0.6	≈ 0	Single
Thin plate [3]	≈ 9	0.4	≈ 0	Single

in the single-domain z-cut configuration has one of the two waveguides under the ground electrode, which induces a lower electro-optic effect due to field spreading compared to the other waveguide under the narrower hot electrode. The result is that the typical driving voltage is about 1.5 times that of a dual-drive structure and 1.4 times that of the proposed geometry.

As an experimental demonstration of this type of modulator, we have fabricated a single-drive Mach-Zehnder interferometer with an active length of $\sim 40 \text{ mm}$. The device is designed according to the previous considerations—see figure 2(c)—and high-voltage ($>10 \text{ kV}$) pulsed poling is performed after Ti-indiffusion on the 0.5 mm thick crystal to obtain the cross-sectional inverted domains.

After DI, the modulator chip undergoes standard fabrication, e.g. silica buffer layer deposition, electroplated thick electrode, etc. In figure 3 we show the microwave reflection coefficient ($|S_{11}|$) and the corresponding electrical

frequency response ($|S_{21}|$). From the figure one can see that the electrical reflection is always below -10 dB and the -6 dB electrical bandwidth is 15 GHz, which also is the expected value for the -3 dB electro-optic bandwidth.

The corresponding switching voltage is $\sim 2 \text{ V}$ (measured at 1 kHz). The modulator could therefore easily be driven with significant extinction by a low-cost driver which typically provides less than 3 V for 10 Gb s^{-1} bit rate, thus allowing the use of inexpensive Si-Ge electro-absorption drivers to modulate. In figure 4 we report the system measurement setup and the eye diagram obtained from a typical low-voltage modulator employing an Inphi 1015EA driver. The eye opening shows a performance suitable for standard optical communication at 10 Gb s^{-1} , including an extinction ratio of 13.65 dB and overall optical losses $<2 \text{ dB}$ at a wavelength of 1550 nm.

3.2. Enhanced bandwidth

The results obtained with domain inversion for the previous modulator contribute to increasing the overlap integral (Γ) without altering BW. In order to increase the bandwidth and the BW/V_{π} ratio even further, we can act on the longitudinal axis of the modulator. The linear response of phase change with length and the fact that higher frequency microwave fields interact with the optical wave over a distance shorter than that of lower frequency fields can be exploited. Indeed, if we consider a VM modulator of length $L = A + B$ with a first non-inverted zone A and a second inverted zone B, the result of the discontinuity in r (in combination with phase velocity matching) is that the device operates in three

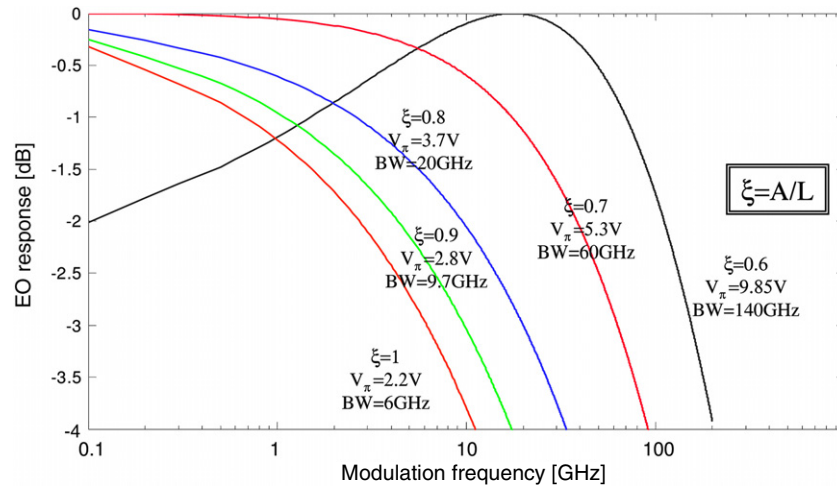


Figure 5. Comparison of electro-optic responses, V_π , and BW for different values of non-inverted to total length $\xi = A/L$.

successive zones along the modulator length. In the upstream zone, desirable phase modulation of the optical wave is induced for all microwave frequencies in the bandwidth of the device. In the middle zone, desirable phase modulation is induced for frequencies in the upper part of the bandwidth, but phase modulation in the lower frequencies becomes excessive. Finally, in the downstream zone, there is no significant phase modulation at higher frequencies, but the excess modulation at lower frequencies is reduced by the fact that the phase modulation has an opposite sign with respect to the upstream and middle zones. In this way the overall phase change of the modulated optical wave can be equalized by properly choosing the lengths A and B . The flattening obtained in the EO response is conceptually similar to the gain flattening operated in an erbium doped fiber amplifier.

In figure 5 we present the comparison between different lengths of the inverted part ($B = L - A$) for a constant interacting length L . Increasing the inverted part leads to a bandwidth broadening and a higher V_π , although the BW/V_π ratio grows at the same time. Thus the geometrical parameters have to be chosen reaching a trade-off between a realistic value for V_π and a desired bandwidth.

As an example, we consider a modulator having a total length $L = 60$ mm, an index mismatch $\delta = 0.05$, with a bandwidth of 30 GHz, and a switching voltage $V_\pi = 4.3$ V with a non-inverted length $A = 47$ mm [17]. The comparison of the performances of the proposed modulator with two classical ones having the same bandwidth or the same voltage respectively imposes the first one to have $L = 26$ mm and $V_\pi = 5.3$ V (BW = 30 GHz), while in the second case $L = 32$ mm and BW = 20 GHz ($V_\pi = 4.3$ V). For the two classical modulators we have $BW/V_\pi = 4.65$, while for the proposed one $BW/V_\pi = 5.66$. The comparison shows that the longitudinal DI modulator has a switching voltage 20% lower for equal bandwidth and a bandwidth 50% larger for equal voltage. Thus, in the proposed design the improvement of BW/V_π figure of merit has been significantly increased at the expense of a longer modulator length, which may be acceptable for those applications not requiring high integration

and where performances are more important than the overall length, as for example in aerospace and defense. Moreover, the viability of the devices is given by the fact that with the actual waveguide fabrication techniques, the increase in optical losses with respect to a standard modulator can be kept below 0.4 dB.

4. Conclusions

We have reported on micro-structured electro-optic waveguide LiNbO₃ modulators which are based on the use of domain inversion in order to enhance the BW/V_π figure of merit. Our work has investigated the impact of using domain inversion engineering for both the longitudinal (along the optical and microwave propagation direction) and transversal modulator sections. We have experimentally demonstrated the feasibility of a modulator with a switching voltage of ~ 2 V and a bandwidth of 15 GHz, suitable for inexpensive ultra low-voltage Si-Ge drivers. Besides, system measurements demonstrate the good performance in terms of extinction ratio (> 13 dB) and wide opening that make the device suitable for 10 Gb s⁻¹ transmission. We have also shown that these performances can be further improved by using a two-section longitudinal domain inversion structure, with an additional potential increase of up to 50% in the electro-optic response figure of merit, at the expenses of overall size.

Acknowledgments

We acknowledge support from the Spanish national programs Plan Nacional No. TEC2007-60185 and Juan de la Cierva.

References

- [1] Wooten L *et al* 2000 *IEEE J. Sel. Top. Quantum Electron.* **6** 69–82
- [2] Alferness R C 1982 *IEEE Trans. Microw. Theory Tech.* **30** 1121–37
- [3] Aoki K, Kondo J, Kondo A, Ejiri T, Mori T, Mizuno Y, Imaeda M, Mitomi O and Minakat M 1982 *J. Lightwave Technol.* **24** 2233–7

- [4] Anwar N, Obayya S S A, Haxha S, Themistos C, Rahman B M A and Grattan K T V 2002 *J. Lightwave Technol.* **20** 826–33
- [5] Garcia Granda M and Hu H 2007 *OptoEL* MOI-13
- [6] Yamada M, Nada N, Saitoh M and Watanabe K 1993 *Appl. Phys. Lett.* **62** 435–6
- [7] Pruneri V, Koch R, Kazansky P G, Russell P St J and Hanna D C 1995 *Opt. Lett.* **20** 2375–7
- [8] Myers L E, Eckardt R C, Fejer M M, Byer R L, Bosenberg W R and Pierce J W 1995 *J. Opt. Soc. Am. A* **12** 2102–16
- [9] Schreiber G, Suche H, Lee Y L, Grundkötter W, Quiring V, Ricken R and Sohler W 2001 *Appl. Phys. B* **73** 501–4
- [10] Schaffner J H 1994 *US Patent Specification* 5,278,924
- [11] Lu Y, Xiao M and Salamo G J 2001 *Appl. Phys. Lett.* **78** 1035–7
- [12] Courjal N, Porte H, Hauden J, Mollier P and Grossard N 2004 *J. Lightwave Technol.* **22** 1338–43
- [13] Lucchi F, Janner D, Belmonte M, Balsamo S, Villa M, Giurgola S, Vergani P and Pruneri V 2007 *Opt. Express* **15** 10739–43
- [14] Janner D, Tulli D, Lucchi F, Vergani P, Giurgola S and Pruneri V 2008 *Appl. Phys. A* **91** 319–21
- [15] Hui K W *et al* 1998 *J. Lightwave Technol.* **16** 232–8
- [16] Haxha S, Rahman B M A and Langley R J 2004 *Opt. Quantum Electron.* **36** 1205–20
- [17] Janner D, Belmonte M and Pruneri V 2007 *J. Lightwave Technol.* **25** 2402–9